Upper Mantle Discontinuity Below the Eastern Alps

Bianchi, I.[1], Miller M. S.[2], Bokelmann, G.[1]

[1] Universität Wien, Institut für Meteorologie und Geophysik, 1090 Wien, Austria
[2] Department of Earth Sciences, University of Southern California, Los Angeles CA 90089-0740, USA

Abstract

Analysis of Ps and Sp receiver functions from datasets collected by permanent and temporary seismic stations, image for the first time lithospheric discontinuities across the entire Eastern Alps with a resolution of tens of kilometers laterally. The receiver functions show the presence of a discontinuity, bounding a low velocity channel, within the upper mantle. The detected discontinuity is deeper (100-130 km) below the central portion of the Eastern Alps, and shallower (70-80 km) towards the Pannonian Basin and in the Central Alps. The comparison renders it likely that the observed discontinuity represents the lithosphere-asthenosphere boundary. This sheds light on the formation and evolution of the Alps, being a result of long-term convergence between the European and Adriatic plates. Previous studies have suggested that the architecture of the eastern portion of the Alpine collision has been affected by lateral (east directed) tectonic extrusion associated with the retreating subduction of the nearby Carpathian slab. Here we confirm with our newly resolved upper mantle discontinuity that both mechanisms are reflected in the structure we image. These new images aid in deciphering and decoupling plate motions from dextral extrusion of the Eastern Alps towards the Pannonian Basin. The lateral variations in lithosphere thickness mirror these two processes and provide us with a better understanding the Alpine tectonics.

STATIONS AND DATA DISTRIBUTION

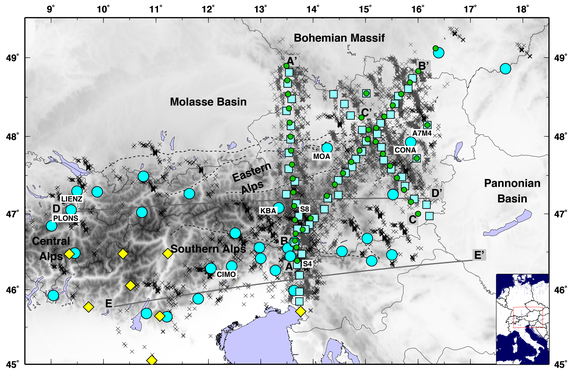

Topographic map of the Eastern Alps, including seismic station locations. Light blue circles show broadband permanent stations from different national networks and squares for temporary stations. Yellow diamonds show stations used in Miller & Piana Agostinetti (2012). Gray crosses are the piercing points at 100 km depth for PRF. Black crosses are piercing points at 100 km for SRF. The inset shows the study area location in Central Europe.

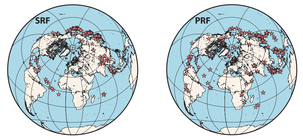

Event distribution at station ACOM for SRFs (154 events), and for S6 from profile BB' for the PRFs (371 events).

METHOD: P- and S- RECEIVER FUNCTION

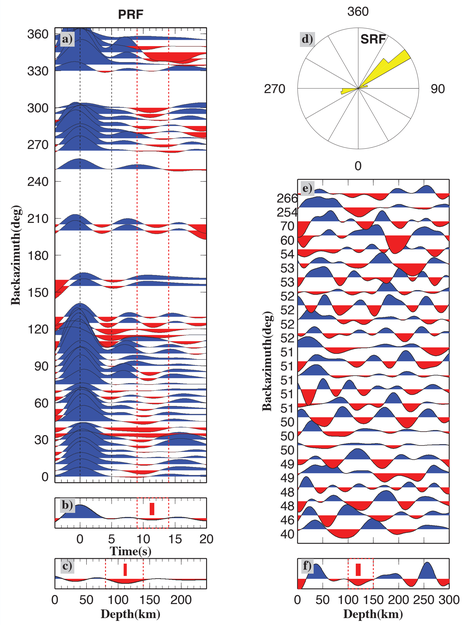

P and S receiver function results evidence for a shallow discontinuity in the mantle below the Eastern Alps. The results for the two different methodologies are strikingly similar.

Here a comparison between P- and SRF datasets computed for data recorded at the station KBA is shown.

a) PRF displayed according to backazimuth.
b) Stack of the PRF from a).
c) Depth migrated stacked PRF.
d) Rose diagram showing the sampled backazimuth directions for teleseisms used to calculate the SRF.
e) SRFs displayed according to the origin backazimuth.
f) Stack of SRFs from e).

Both data-set show a velocity inversion in the upper mantle.
The velocity inversion depth estimate is 112 km for the stacked PRFs, and 120 km for the SRFs.

DATA ALONG PROFILE SHOW DEPTH VARIATIONS

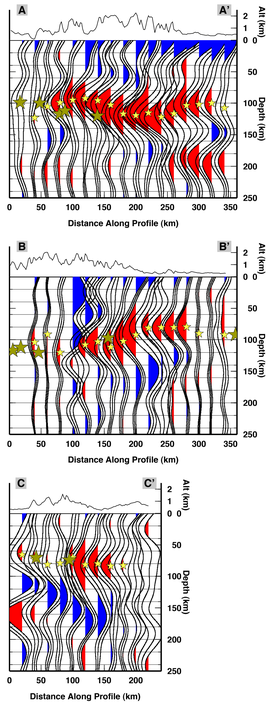

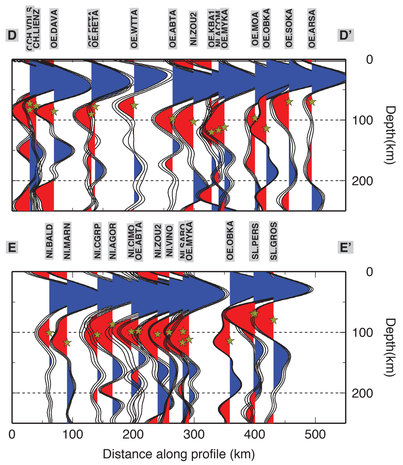

SRF stacks for the permanent stations along profiles DD' and EE'. Stars indicate the interpreted discontinuity depth at each station.
SRF were computed following the methodology described in detail in Levander and Miller (2012).

PRF common-conversion-point profiles migrated at 100 km depth along profiles AA', BB' and CC'. Green stars for discontinuity depth from the SRFs at adjacent stations. Yellow stars indicate the interpreted discontinuity depths from the PRFs.

P receiver functions have been calculated with a frequency domain algorithm using multitaper correlation estimates (Park and Levin, 2000) with a frequency cut off of 0.2 Hz.

Using both SRF and PRF analyses, we detect a negative impedance contrast generated atop of a low velocity layer in the upper mantle, that likely corresponds to the bottom of the lithosphere (lithosphere-asthenosphere boundary or LAB).

The dense distribution of temporary stations allows for the identification of lateral depth variations over length scales of several tens of kilometers, and are supported by depth estimates from permanent stations. We image the deepening of a low velocity channel in the central Alps, and its rise towards the east.

LITHOSPHERE THICKNESS

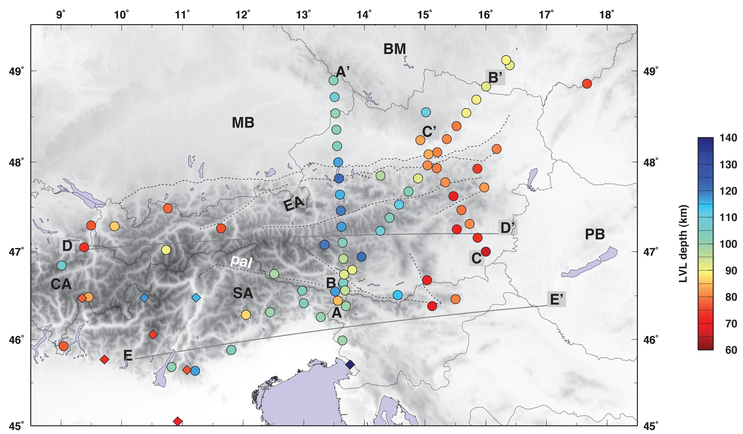

Lithosphere thickness under the Eastern Alps. Circles for depths inferred from this study, diamonds for depths from Miller and Piana Agostinetti 2012. pal= periadriatic line.

Variations in lithospheric thickness occur over length scales of several tens of kilometers beneath the Alpine chain. The thicker lithosphere is affected by the presence of the downgoing slab, and in the farthest eastern Alps the lithosphere is thinned by the dextral extrusion of the Eastern Alps towards the Pannonian Basin.

COMPARISON WITH OTHER OBSERVATIONS

Interpreted lithosphere thickness compared to a) Moho depths and plate boundaries from Brückl et al (2010) , where PA is the Pannonian plate, EU is the Eurasian plate, and AD is the Adriatic plate. b) tomographic anomalies from Lippitsch et al. (2003). c) SKS splitting directions are shown as pink bars (Bokelmann et al. 2013) and black bars (Wustefeld et al., 2009). d) Surface heatflow (Artemieva et al. 2006).

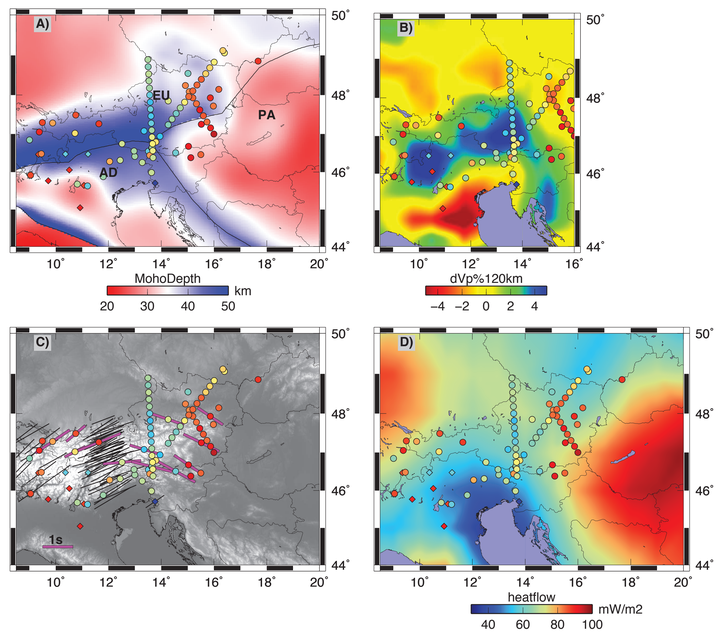

SUMMARY

Both Ps and Sp converted energy independently confirm the existence of a discontinuity that correlates with the lithosphere-asthenosphere boundary. PRF offer a valid support to the SRF results in those areas where permanent stations are lacking.

This study adds details and points out the depth variations of the lithosphere system: EA: ~120-130 km depth; SA: ~100-110 km depth; MB: ~100 km depth; BM: ~90km depth; CA:~ 80-90 km depth; PB: ~70-80 km depth.

Depth variation reflect the depth extent of the eastward extrusion of the EA towards the Pannonian Basin.

REFERENCES

Artemieva, I.M., Thybo, H., Kaban, M.K. Deep Europe today: Geophysical synthesis of the upper mantle structure and lithospheric processes over 3.5 Ga (2006) Geological Society Memoir, 32, pp. 11-41. **Bokelmann**, G., Qorbani Chegeni, E., Bianchi, I., 2013, Seismic Anisotropy and Large-Scale Deformation of the Eastern Alps, Earth and Planetary Science Letters, doi:10.1016/j.epsl.2013.09.019. **Brückl**, E., Behm, M., Decker, K., Grad, M., Guterch, A., Keller, G. R., Thybo, H. (2010), Crustal structure and active tectonics in the Eastern Alps, Tectonics 29 (2). **Lippitsch**, R., Kissling, E., Ansorge, J. (2003), Upper mantle structure beneath the alpine orogen from high-resolution teleseismic tomography, J. Geophys. Res 108 (2376). **Levander**, A. and Miller, M.S., (2012), Evolutionary aspects of lithosphere discontinuity structure in the western U.S., Geochemistry, Geophysics, Geosystems, 13, doi:10.1029/2012GC004138. **Miller**, M. S. Piana Agostinetti N. 2012. Insights into the evolution of the Italian lithospheric structure from S receiver function analysis. Earth and Planetary Science Letters, Volumes 345–348, September 2012, Pages 49-59. **Park**, J., Levin, V., 2000. Receiver functions from multiple-taper spectral correlation estimates. Bull. Seismo. Soc Amer. 90, 1507–1520. **Wüstefeld**, A.; Bokelmann, G. H. R.; Barruol, G.; Montagner, J.-P. (2009) "Identifying global seismic anisotropy patterns by correlating shear-wave splitting and urface waves data" , Phys. Earth Planet. Int, 176 (3-4), 198-212, doi:10.1016/j.pepi.2009.05.006.